Linear and Nonlinear Optical Properties of [60]Fullerene Derivatives

O. Loboda,[a] R. Zaleśny,[a,b] A. Avramopoulos,[a] J. –M. Luis,[c] B. Kirtman,[d] N. Tagmatarchis,[e] H. Reis,[a] and M. G. Papadopoulos,[a,‡]

[a] *Institute of Organic and Pharmaceutical Chemistry,*
The National Hellenic Research Foundation,
48 Vas. Constantinou Avenue, 11635 Athens, Greece
[b] *Institute of Physical and Theoretical Chemistry,*
Wroclaw University of Technology, Wyb. Wyspiańskiego 27,
50–370, Wrocław, Poland
[c] *Institute of Computational Chemistry, University of Girona,*
Campus de Montilivi, 17071 Girona, Catalonia, Spain
and Department of Chemistry, University of Girona,
Campus de Montilivi, 17071 Girona, Catalonia, Spain
[d]*Department of Chemistry and Biochemistry, University of California,*
Santa Barbara, California 93106, USA
[e] *Theoretical and Physical Chemistry Institute,*
The National Hellenic Research Foundation,
48 Vas. Constantinou Avenue, 11635 Athens, Greece
[‡] *Corresponding author: mpapad@eie.gr*

September 15, 2008

1 Abstract

Using a wide variety of quantum–chemical methods we have analyzed in detail the linear and non–linear optical properties of [60]fullerene–chromophore dyads of different electron–donor character. The dyads are composed of [60]fullerene covalently linked with 2,1,3–benzothiadiazole and carbazole derivatives. Linear scaling calculations of molecular polarizabilities were performed using wave function theory as well as density functional theory (DFT). Within the former approach, we used both semiempirical (PM3) and *ab initio* (Hartree-Fock and second–order Møller–Plesset perturbation theory) methods. Within the latter approach only the recently proposed long–range (LRC) schemes successfully avoid a large overshoot in the value obtained for β. Calculations on model fullerene derivatives establish a connection between this overshoot and the electron–donating capability of the substituent.

Substitution of 2,1,3–benzothiadiazole by the triphenylamine group significantly increases the electronic first and second hyperpolarizabilities as well as the two–photon absorption cross section. For [60]fullerene–chromophore dyads we have, additionally, observed that the double harmonic vibrational contribution to the static β is much larger than its electronic counterpart. Although the vibrational term is reduced in magnitude, the same is true for the dc–Pockels β as compared to the static electronic value. A nuclear relaxation treatment of vibrational anharmonicity for a model fulleropyrrolidine molecule yields a first–order contribution that is substantially more important than the double harmonic term.

2   Introduction

During recent years significant progress has been made in the synthesis and characterization of photoactive materials.[1] In particular, tremendous efforts have been invested in the design of materials exhibiting high nonlinear optical response. A plethora of organic[2,3] and organometallic[4,5] systems have been studied in this context.

One of the most common strategies for design of new molecules with high values of the first hyperpolarizability (β) has its roots in the so called two–state model proposed in the late seventies.[6] Within this model, β is expressed in terms of the dipole moment difference, transition dipole moment and energy difference between the key charge transfer excited state and the ground electronic state. Numerous molecular systems of diverse donor–acceptor (DA) character have been proposed according to the two–level model in order to maximize β.

[60]Fullerene is an especially interesting acceptor molecule. When combined with photo– and/or electro–active moieties an efficient charge separation and slow charge recombination occurs due to its small reorganization energy. Many [60]fullerene–based hybrid materials with porphyrins,[7] tetrathiafulvalenes[8] and ferrocenes[9] have been prepared and studied in the past. Recently, several dyad systems wherein [60]fullerene is combined with the carbazole, benzothiazole and benzothiazole–triphenylamine moieties have been synthesized[10,11] (**1–3** in Figure 1, respectively) with an eye towards their potential usefulness as photonic materials. The primary goal of the present contribution is to calculate and analyze the nonlinear optical properties of these dyad systems.

Each of the chromophores mentioned above is interesting in its own right. Carbazole is an organic compound which exhibits unusual photophysical properties, such as the photoconductivity observed in poly–vinyl–carbazole.[12] On the other hand, 4,7–diphenyl–2,1,3–benzothiazole-based compounds are strongly fluorescent dyes,[13,14] which have absorption and emission profiles that can be easily tuned by substitution at the aryl unit of the benzothiazole moiety. Finally, triphenylamine (TPhA) based materials are widely known as excellent hole–transporters and electroluminescent components;[10,11,15] films of TPhA have been used in organic–light–emitting–diodes (OLEDs).[16] In all three dyad systems a pyrrolidine unit is incorporated into the skeleton of the [60]fullerene (using the well–established 1,3-dipolar cycloaddition reaction of azomethine ylides[17]). Here we study how modification of the chromophore influences the non–resonant first and second hyperpolarizability.

Apart from non–resonant properties, resonant two–photon absorption (TPA) is also of interest. Although TPA was predicted by Maria Göppert–Mayer in the early 1930's,[18] it has only recently attracted significant attention.[19–27] This is due to various optical applications, including optical limiting[28] and optical data storage.[29] Based on numerous theoretical and experimental investigations, certain structure–property relationships have been established for TPA in conjugated organic molecules.[19,20,26] However, only a small number of studies have been devoted to functionalized fullerenes.[30] It has been observed experimentally that TPA cross sections of [60]fullerene–chromophore dyads can be as large as 10^4 GM (1 GM $= 1 \cdot 10^{-50}$ cm^4·s·photon^{-1}·molecule^{-1}).[31] However, the measurements were performed with pulses of nanosecond duration and the observed TPA includes contributions from secondary processes.[31] Hence, we also want to calculate and analyze the TPA of **1**, **2**, **3** as a function of wavelength.

The performance of various theoretical approaches for calculation of nonlinear optical properties has been examined extensively.[32] It is desirable to apply coupled cluster methods wherever possible.[33] However, this level of theory is not a practical choice for large systems.

Even the computationally less intensive MP2 method is too demanding for the systems under consideration here except for benchmarking purposes. An alternative is density functional theory, which accounts for electron correlation much more efficiently than wavefunction treatments. It has been recognized, however, that the majority of exchange–correlation functionals fail to correctly predict polarizabilities and hyperpolarizabilities of chain–like molecules.[34,35] Long–range corrected (LRC) functionals have been proposed recently to alleviate this deficiency. In this article, we shall refer to such methods as LRC–DFT and, in particular, we will examine the suitability of the LC–BLYP[36–38] and CAM–B3LYP[39] variants for the systems/properties at hand. LRC-DFT has been used to calculate nonlinear optical properties for a number of systems[37,38,40–42] but we are not aware of any studies on organofullerenes. More conventional functionals are also used for comparison purposes.

In the present contribution we compute both electronic (Sec. 4.2) and vibrational (Sec. 4.4) contributions to the non–resonant (hyper)polarizability of the [60]fullerene derivatives mentioned above and study their one– and two–photon absorption as well. We also relate these linear and nonlinear optical properties to their electronic structure (sec. 4.3) in order to build a basis for the rational design of new [60]fullerene derivatives suitable for photonic applications.

3   Computational Methods

Geometry optimizations were performed using the semiempirical PM3 Hamiltonian[43,44] and the B3LYP/6-31G(d) method. All stationary points were confirmed to be minima by evaluation of the hessian. The calculation of the linear and nonlinear optical properties is described in the following sub–sections. In order to speed up computations the fast multipole method (FMM)[45–47], as implemented in Gaussian 03,[48] has been used wherever applicable.

3.1   Definition of static electric dipole properties

In the presence of moderate uniform static electric fields, in one or more Cartesian directions, the total molecular energy can be expressed as a Taylor series:

$$E(F) = E(0) - \mu_i F_i - \frac{1}{2!}\alpha_{ij}F_iF_j - \frac{1}{3!}\beta_{ijk}F_iF_jF_k - \frac{1}{4!}\gamma_{ijkl}F_iF_jF_kF_l - \dots, \qquad (1)$$

where $E(0)$ denotes the energy without external perturbation; the Greek symbols $\alpha, \beta \dots$, label tensor quantities; and the subscripts indicate cartesian directions. This expansion (1) conforms to the so–called T–convention[49] and is employed here for determination of the static linear polarizability (α), first hyperpolarizability (β) and second hyperpolarizability (γ). The average (hyper)polarizabilities are defined in the following way:[32]

$$\overline{\alpha} = \frac{1}{3}\sum_{i=x,y,z}\alpha_{ii}, \qquad (2)$$

$$\overline{\beta} = \sum_{i=x,y,z}\frac{\mu_i\beta_i}{|\mu|}, \qquad (3)$$

where

$$\beta_i = \frac{1}{5}\sum_{j=x,y,z}\left(\beta_{ijj} + \beta_{jij} + \beta_{jji}\right), \qquad (4)$$

and

$$\overline{\gamma} = \frac{1}{5}\sum_{ij=x,y,z}\gamma_{iijj}. \qquad (5)$$

Within the clamped nucleus approximation, the (hyper)polarizabilities can be divided into two parts, namely electronic and vibrational:[50]

$$P = P^e + P^{vib}, \tag{6}$$

with[51]

$$P^{vib} = P^{nr} + P^{curv}. \tag{7}$$

Here we compute the nuclear relaxation contribution, P^{nr}, to α^{vib} and β^{vib}. This term can be identified with lower–order vibrational perturbation theory contributions based on a double harmonic (mechanical, electrical) zeroth–order model. $P^{(nr)}$ is typically the larger of the two terms on the right hand side of Eq. (7). In the above partitioning scheme the zero–point vibrational averaging contribution is part of the curvature term, P^{curv}. It is usually quite small and is not computed here.

3.2   Static electronic contributions

Numerical differentiation of the total energy with respect to the static electric field(s), at the equilibrium geometry, allows for determination of the electronic contribution to the expansion coefficients in (Eq. (1)). The diagonal tensor components, for example, can be determined as:[52]

$$\mu_i F_i = -\frac{2}{3}[E(F_i) - E(-F_i)] + \frac{1}{12}[E(2F_i) - E(-2F_i)], \tag{8}$$

$$\alpha_{ii} F_i^2 = \frac{5}{2} E(0) - \frac{4}{3}[E(F_i) + E(-F_i)] - \frac{1}{12}[E(2F_i) + E(-2F_i)], \tag{9}$$

$$\beta_{iii} F_i^3 = [E(F_i) - E(-F_i)] - \frac{1}{2}[E(2F_i) + E(-2F_i)], \tag{10}$$

$$\gamma_{iiii} F_i^4 = -6E(0) + 4[E(F_i) + E(-F_i)] - [E(2F_i) + E(-2F_i)]. \tag{11}$$

Although numerical calculation of μ and α strictly requires only two field–dependent energies, the use of four points as in Eq.(8) reduces numerical error. It is also possible to use the expansion of the dipole moment for calculation of α, β and γ. Nevertheless, in the great majority of calculations presented herein, we used expansion (1). In a few cases, diagonal components of the hyperpolarizability were calculated as a derivative of the analytical α with respect to electric field. The Romberg procedure was used to check the validity of the finite–field results.[53]

Calculations of the electronic contribution to (hyper)polarizabilities using Hartree–Fock and second–order Møller–Plesset perturbation theory (MP2) were performed using the Gaussian 03 program[48], while for the semiempirical calculations we used the MOPAC 2007 package.[54] Density functional theory computations were performed using Gaussian 03 (B3LYP, PW91, LDA),[48] ADF (current DFT, LB94, RevPBEx, GRAC, KT1, KT2, KLI),[55] Dalton (CAM–B3LYP)[56], and GAMESS US (LC–BLYP).[57] We used linear scaling approaches for calculations of nonlinear optical properties as implemented in the ADF package.[55] All properties are expressed in atomic units. Conversion factors can be found elsewhere.[32]

3.3   Vibrational contributions

In order to compute vibrational nuclear relaxation (NR) contributions, the field induced coordinates (FICs) approach has been employed.[58,59] The FICs are linear combinations of field-free normal coordinates associated with the change in equilibrium geometry induced by

a static electric field. The value of the ith field–free normal coordinate at the field–relaxed geometry is given by:[58]

$$Q_i^F(F_x, F_y, F_z) = -\sum_a^{x,y,z} q_1^{i,a} F_a - \sum_{a,b}^{x,y,z} \left[q_2^{i,ab} - \sum_{j=1}^{3N-6} \frac{a_{21}^{ij,a}}{a_{20}^{ii}} q_1^{i,b} + \sum_{j,k=1}^{3N-6} \frac{3a_{30}^{ijk}}{2a_{20}^{ii}} q_1^{j,a} q_1^{k,b} \right] F_a F_b + \ldots, \tag{12}$$

where,

$$a_{nm}^{ij\ldots ab\ldots} = \frac{1}{n!m!} \left(\frac{\partial^{(n+m)} V(Q_1, \ldots, Q_{3N-6}, F_x, F_y, F_z)}{\partial Q_i \partial Q_j \cdots \partial F_a \partial F_b \cdots} \right)_{Q=0, F=0}, \tag{13}$$

and

$$q_1^{i,a} = \frac{a_{11}^{i,a}}{2a_{20}^{ii}}, \qquad q_2^{i,ab} = \frac{a_{12}^{i,ab}}{2a_{20}^{ii}}. \tag{14}$$

Here, in order to conform to standard practice, the indices i, j, k label normal coordinates whereas a, b, c now refer to cartesian directions along molecular axes. This should not cause any confusion since we will use the Cartesian directions x, y, z to report our results. The quantities a_{nm} involve the nth derivative of the potential energy $V(Q, F)$ with respect to normal coordinates and the mth derivative with respect to field components. In terms of these quantities the first– and second–order FICs are defined as:[58]

$$\chi_1^a = -\sum_{i=1}^{3N-6} q_1^{i,a} Q_i, \tag{15}$$

and

$$\chi_2^{ab} = -\sum_{i=1}^{3N-6} \left[q_2^{i,ab} - \sum_{j=1}^{3N-6} \frac{a_{21}^{ij,a}}{a_{20}^{ii}} q_1^{j,b} + \sum_{j,k=1}^{3N-6} \frac{3a_{30}^{ijk}}{2a_{20}^{ii}} q_1^{j,a} q_1^{k,b} \right] Q_i. \tag{16}$$

Depending on the NLO property of interest, a small set of FICs, independent of the number of atoms in the molecule, may be employed to calculate the total NR contribution which would be obtained using all $3N$-6 normal coordinates. For example, from the three first–order FICs (one for each cartesian direction) one can compute the nuclear relaxation contributions to the static polarizability and first hyperpolarizability, as:

$$\alpha_{ab}^{nr}(0;0) = \frac{1}{2} \sum P_{ab} \frac{\partial \mu_a}{\partial \chi_1^b} \frac{\partial \chi_1^F}{\partial F_b} = [\mu^2]^{(0,0)}, \tag{17}$$

$$\begin{aligned} \beta_{abc}^{nr}(0;0,0) &= \sum P_{abc} \left[\frac{1}{2} \frac{\partial \alpha_{ab}}{\partial \chi_1^c} \frac{\partial \chi_1^F}{\partial F_c} + \frac{\partial^2 \mu_a}{\partial \chi_1^b \partial \chi_1^c} \frac{\partial \chi_1^F}{\partial F_b} \frac{\partial \chi_1^F}{\partial F_c} - \frac{1}{6} \frac{\partial^3 V}{\partial \chi_1^a \partial \chi_1^b \partial \chi_1^c} \frac{\partial \chi_1^F}{\partial F_a} \frac{\partial \chi_1^F}{\partial F_b} \frac{\partial \chi_1^F}{\partial F_c} \right] \\ &= [\mu\alpha]^{(0,0)} + [\mu^3]^{(1,0)} + [\mu^3]^{(0,1)}, \end{aligned} \tag{18}$$

where $\sum P_{ab\ldots}$ indicates the sum over all permutations of the indices $a, b, \ldots$ The superscripts in the last line of Eq. (18) denote the order (in perturbation theory) of electrical and mechanical anharmonicity, respectively.[60] It is also possible, using only first–order FICs, to compute the NR contribution to the frequency–dependent Pockels effect (dc–P) $\beta(-\omega; \omega, 0)$ and electric field induced second–harmonic generation (EFISH) $\gamma(-2\omega; \omega, \omega, 0)$ in the infinite optical frequency ($\omega \to \infty$) approximation. In the latter approximation the first-order corrections vanish and we are left with a double harmonic term. The same is true of the intensity–dependent refractive index (IDRI) $\gamma(-\omega; \omega, -\omega, \omega)$. More details about this method can be found elsewhere.[58,59,61]

The potential energy and electrical properties in Eqs. (17) and (18) were computed using

195 the Gaussian 03 program.[48] Derivatives with respect to the FIC coordinate were obtained
196 numerically, at the field–free optimum geometry, by applying a number of steps along the
197 FIC vector. This was done for molecule **8**. In other cases, the nuclear relaxation contribu-
198 tions were estimated based on the double–harmonic oscillator approximation (which is exact
199 for α, dc-P, and IDRI),[32,62] *i.e.* for β only the $[\mu\alpha]^{(0,0)}$ term was evaluated, and, in that
200 event, the GAMESS US package was employed.[57] In calculating vibrational contributions
201 at a given level of theory we were careful to use the geometry optimized by the very same
202 method.

3.4   One– and Two–photon absorption (TPA)

204 The quantity needed to describe the simultaneous absorption of two photons which, in
205 general, have different energies ($\hbar\omega_1 \neq \hbar\omega_2$) and different polarization ($\vec{\zeta_1} \neq \vec{\zeta_2}$) is given by
206 the following equation:[63]

$$S_{ij}^{0F}(\vec{\zeta_1},\vec{\zeta_2}) = \hbar^{-1} \sum_K \left[\frac{\langle 0|\vec{\zeta_1} \cdot \hat{\mu}_i|K\rangle\langle K|\vec{\zeta_2} \cdot \hat{\mu}_j|F\rangle}{\omega_K - \omega_1} + \frac{\langle 0|\vec{\zeta_2} \cdot \hat{\mu}_i|K\rangle\langle K|\vec{\zeta_1} \cdot \hat{\mu}_j|F\rangle}{\omega_K - \omega_2} \right] \quad (19)$$

207 Here $\hbar\omega_1 + \hbar\omega_2$ should satisfy the resonance condition $\omega_F = \omega_1 + \omega_2$ and $\langle K|\vec{\zeta_1} \cdot \hat{\mu}|L\rangle$
208 is the transition moment between electronic states K and L, respectively. Since in most
209 experiments one source of photons is used, one can substitute $0.5 \cdot \omega_F$ for the angular
210 frequencies ω_1 and ω_2 . In the case of isotropic media the averaged two–photon absorption
211 cross section is given by:

$$\langle \delta^{0F} \rangle = \frac{1}{30} \sum_{ij} \left[S_{ii}^{0F}(S_{jj}^{0F})^* \bar{F} + S_{ij}^{0F}(S_{ij}^{0F})^* \bar{G} + S_{ij}^{0F}(S_{ji}^{0F})^* \bar{H} \right] \quad (20)$$

212 where $\bar{F} = \bar{F}(\bar{\zeta_1},\bar{\zeta_2})$, $\bar{G} = \bar{G}(\bar{\zeta_1},\bar{\zeta_2})$, and $\bar{H} = \bar{H}(\bar{\zeta_1},\bar{\zeta_2})$ are the polarization variables. For
213 two linearly polarized photons with parallel polarization, $\bar{F},\bar{G},\bar{H}$=2 and the two–photon
214 absorption cross–section is:[63]

$$\langle \delta^{0F} \rangle = \frac{1}{15} \sum_{ij} \left[S_{ii}^{0F} (S_{jj}^{0F})^* + 2S_{ij}^{0F}(S_{ij}^{0F})^* \right]. \quad (21)$$

215 The comparison of the theoretically determined two–photon absorption cross section with
216 experimental spectra is based on the relation:

$$\sigma_{0F}^{(2)} = \frac{8\pi^3\alpha^2\hbar^3}{e^4} \frac{\omega^2 g(\omega)}{\Gamma_F/2} \langle \delta^{0F} \rangle, \quad (22)$$

217 where e is the magnitude of the electronic charge, α is the fine structure constant (not to
218 be confused with the linear polarizability), $\hbar\omega$ is the energy of absorbed photons (assuming
219 single source of photons), Γ_F is the lifetime broadening of the final state and $g(\omega)$ is the
220 spectral line profile, which is assumed here to be a δ–function. The quantities on the right
221 hand side of Eq.(19) were obtained from single excitation configuration interaction (CIS)
222 calculations using the GRINDOL method[79], which is based on the INDO approximation,
223 with 2000 singly excited configurations. The same GRINDOL calculation also yields the
224 quantities needed to obtain the one–photon absorption spectrum. As shown previously, the
225 GRINDOL/CIS level of theory correctly predicts both one–photon spectra and nonlinear
226 optical properties of donor–acceptor systems.[64,65] Although a theoretical treatment of the
227 vibrational contribution to TPA has been developed[66] we have not attempted to apply it
228 here.

4   Results and discussion

230 This section is organized as follows. Firstly, we shall discuss the structure of the investigated
231 systems (Sec. 4.1). Then the electronic contributions to linear polarizability, and first and

232 second hyperpolarizability are presented in Sec. 4.2. In the following section we analyze
233 one– and two–photon absorption spectra (Sec. 4.3) and, finally, the discussion of vibrational
234 contributions to the (hyper)polarizabilities is given in Sec. 4.4.

4.1 Structure of investigated molecules

236 *Ab initio* calculation of optimized geometries for the systems investigated here is compu-
237 tationally demanding, especially since we want to evaluate the hessian to confirm that the
238 stationary point is a minimum. Thus, the semiempirical PM3 method was used for this
239 purpose. In order to assess the reliability of the PM3 structures, we optimized the geometry
240 of **1** (Figure 2) at the B3LYP/6-31G(d) level of theory as well. The comparison of PM3 and
241 B3LYP results reveals only minor changes in the bond distances of the fullerene moiety, *i.e.*
242 the carbon–carbon (hexagon–pentagon) and (hexagon–hexagon) bond length differences do
243 not exceed 0.01 Å and 0.012 Å, respectively. The values of selected geometrical parameters
244 for **1** are listed in Table 1. They are in reasonable agreement. Perhaps the most significant
245 difference between PM3 and B3LYP/6-31G(d) occurs for the N'–CH_3 group of the carbazole
246 moiety. Fortunately, this difference does not have a significant effect on the linear and non-
247 linear optical properties as seen below. No experimental structure is available for **1**.
248
249 In Table 2 we present values for the electronic dipole moments and average (hyper)polariza-
250 bilities of **1** calculated at the HF/6-31G(d) level of theory for the structures obtained by the
251 two methods discussed above. The difference in property values is not substantial as far as
252 the purposes of this study are concerned. Thus, the structures of all investigated molecules
253 were optimized using the PM3 method, except for evaluation of vibrational contributions to
254 α and β, in which case the structure and property derivatives must be obtained by the same
255 method as previously noted. It should be mentioned that we consistently use the so–called
256 standard orientation[69] which is presented for molecules **1**–**3** in Figure 2.

4.2 Electronic contributions to (hyper)polarizabilities

258 In this section, we discuss the electronic contributions to α, β and γ. In particular, two
259 aspects will be considered in detail: (1) the reliability of DFT results obtained using various
260 exchange–correlation functionals and (2) the relation between the structure and non–linear
261 optical properties of the molecules studied here.
262
263 Our calculated results for the largest diagonal, *i.e.x*, component of the static μ, α, and
264 β of molecule **1** are presented in Table 3 for various DFT functionals; HF and MP2 val-
265 ues are also given for comparison. The DFT functionals were tested using either a 3-21G
266 or DZP basis. It is now well–recognized that conventional functionals tend to strongly
267 overshoot the magnitude of longitudinal electrical property values in conjugated chain–like
268 molecules.[34,35,70–72] Hence, the very large values, compared to Hartree–Fock or MP2 or the
269 (non-conventional) CAM–B3LYP and LC–BLYP functionals, as reported in Table 3, should
270 probably not be surprising. The overshoot for β is especially noticeable. Although the DZP
271 basis is not quite the same as 6-31G(d) they are similar enough to make valid comparisons.
272
273 As far as the non–conventional functionals are concerned, KLI[73] has been found to yield
274 substantial improvement for α and γ of molecular hydrogen chains[70] with bond length al-
275 ternation, although deficiencies still remain in comparison to, say, the optimized effective
276 potential (OEP).[76] Since OEP is, in principle, equivalent to Hartree–Fock, we can compare
277 with the latter. In that event the overshoot we obtain for the KLI β is quite striking. The
278 non–conventional current–DFT (cDFT) approach[74] has previously proved successful for α
279 of π–conjugated molecules,[72]. However, it has difficulty in this case with μ and, especially,
280 with β. On the other hand, the recently developed LRC functionals CAM–B3LYP[39] and

281 LC-BLYP[36-38], which use exact Hartree–Fock exchange at long–range together with more
282 conventional functionals at short range, successfully cure the overshoot problem.

283

284 Judging by the comparison between Hartree–Fock and MP2 (as well as the two LRC func-
285 tionals) the effect of electron correlation on β appears to be important. This is consistent
286 with what has been found for a number of charge transfer molecules. Extending the basis
287 set from 3-21G to 6-31G(d) has a smaller, though still significant, effect on both the HF and
288 MP2 values of β.

289

290 In order to investigate the connection between the overshoot for β obtained by conven-
291 tional DFT and the donor–acceptor character of the dyad, we performed calculations for
292 several systems containing a simple donor group (or two) (see Table 4) attached to the
293 [60]fullerene moiety. Although these systems may not adequately model molecules **1-3** the
294 results turn out to be very suggestive. In these calculations BLYP was used as a repre-
295 sentative conventional functional and comparison was made to HF, which does not suffer
296 from the overshoot problem. The additive substituents were selected according to increasing
297 Hammett σ_p constant which may be used as a measure of their electron donating capabilities.

298

299 Based on the data in Table 4, one fact clearly emerges. For the sequence of molecules
300 **9**, **10**, **12** and **14**, ordered according to increasing Hammett σ_p of the additive substituent,
301 the ratio of the BLYP and HF values for $\overline{\beta}$ increases monotonically and becomes quite large
302 for the strongest donors. Furthermore, a very similar pattern is seen for the doubly substi-
303 tuted [60]fullerene derivatives.

304

305 The results of calculations for the static electric dipole properties of molecules **1**, **2** and
306 **3** are presented in Table 5. Our aim here is to validate the PM3 procedure. For this pur-
307 pose, we focused on the diagonal x–component. This component is the the largest for α, β,
308 and γ, though not necessarily for μ. The overall agreement between PM3 and LC–BLYP/3-
309 21G is satisfactory from our point of view and both procedures are reasonably consistent
310 with MP2/3-21G. As implied above this will not be altered by choosing a larger basis set.
311 Thus, we shall use values of $\overline{\alpha}$, $\overline{\beta}$ and $\overline{\gamma}$ calculated using PM3 as the basis for further analysis.

312

313 PM3 values for the averaged static electric properties of **1**, **2** and **3** are shown in Table
314 6 along with the corresponding isolated chromophores **5**, **6** and **7**, respectively. The chro-
315 mophore dyad values are considerably larger although, as might be expected, this effect
316 decreases as the length of the isolated chromophore increases. Nonetheless the general
317 trends for both sets of molecules parallel one another. In both cases the magnitude of $\overline{\beta}$ is
318 similar for **1** (**5**) and **2** (**6**) while the value for **3** (**7**) is much larger. For $\overline{\alpha}$ and $\overline{\gamma}$ there is a
319 systematic increase along the sequence: **1** → **2** → **3** (**5** → **6** → **7**).

320 4.3 One– and two–photon absorption spectra

321 One– and two– photon absorption spectra were calculated using the GRINDOL[79] CIS
322 method as described in Sec. 3.4. This technique has been proven to provide reliable predic-
323 tion of one–photon spectra of organic compounds.[80] Theoretically determined one–photon
324 spectra of isolated **1**, **2**, **3** and **4** are presented in Fig. **??**. The spectrum of **4** measured in
325 cyclohexane by Maggini *et al.*[81] is also presented in Fig. 3. Our semiempirical calculations
326 (without solvent correction) agree fairly well with the experimental data.

327

328 Comparison of spectra of **4** and **1** reveals the existence of a very intense peak (oscilla-
329 tor strength greater than 0.6) in the spectrum of **1**,located at 262 nm, which is not present
330 in the spectrum of **4**. An analysis of the CI vectors reveals that this is a $\pi \rightarrow \pi^*$ transition
331 that occurs in the pyrrolidine ring of the carbazole moiety.

332

333 In the case of compounds **2** and **3** one obtains very intense transitions at 412 and **309**
334 nm for **2** and 418 and 323 nm for **3**. The calculated absorption band maxima for **3** are in
335 good agreement with the experimental values of 436 nm and 310 nm for the chromophore
336 in CH_2Cl_2.[14] The authors attributed these to intramolecular $\pi \to \pi^*$ transitions from the
337 TPhA (donor) to the benzothiadiazole (acceptor) moiety.[14] The results of our calculations
338 fully support this assignment. No experimental data has been reported for compound **2**.

339

340 For molecule **3** we also calculated one–photon spectra with the aid of time–dependent density
341 functional theory using B3LYP functional and 6-31G(d) basis set. The most intense tran-
342 sition is predicted at 2.186 eV (567 nm), which is significantly shifted to higher wavelength
343 from both the measured and GRINDOL values. The large disagreement with experiment is
344 consistent with the fact that charge transfer excitations are poorly described by B3LYP cal-
345 culations.[40] Finally, we note that the spectrum below 250 nm is connected with excitations
346 localized mainly in the [60]fullerene moiety as may be seen by comparing with our Fig. 3
347 which also contains the experimental data reported by Maggini *et al.*[81] The same is true for
348 the other three molecules.

349

350 Figure 4 presents the dipole moment components of **1**, **2** and **3** in their ground state as
351 well as in selected excited states. The dipole moments were calculated as expectation val-
352 ues based on the CIS wavefunction of a given singlet excited state determined using the
353 GRINDOL method. The computations were performed for molecules oriented as presented
354 in Fig. 2 (see also Fig. 2). We include only states for which $|\Delta\mu| = |\mu_e - \mu_g| > 2$ D (0.787
355 au) and f > 0.05, where f, μ_e and μ_g denote oscillator strength, excited state and ground
356 state dipole moment, respectively. In cases where a single charge–transfer state is dominant
357 the quantities $|\Delta\mu|$ and f are the key parameters determining the first hyperpolarizability[6]
358 as well as the two–photon absorption cross section.[84] From the figure we see that it is
359 the x component of $|\Delta\mu|$ that achieves particularly large values. That component points
360 in the same direction (*i.e.* from the [60]fullerene moiety towards the chromophore) for **1**,
361 **2**, and **3**. We also present in Fig. 4 the ground state dipole moment components for the
362 chromophores **5**, **6** and **7** at the same orientation. By comparing the chromophore to the
363 corresponding dyad it is clear that the [60]fullerene serves as an electron withdrawing moiety
364 in the ground state of all three molecules. On the other hand, the [60]fullerene moiety can
365 act as an electron–donating group in excited states.[85] Indeed, it is seen from Fig. 4, that
366 in some excited states of **1**, **2** and **3**, the x component of the dipole moment changes sign
367 and has a large increase in magnitude. This is indicative of the fact that the [60]fullerene
368 moiety is donating electrons to the carbazole–based and 2,1,3–benzothiadiazole–based units.

369

370 The two–photon absorption spectra of the investigated molecules is presented in Fig. **??–??**.
371 These plots were prepared assuming that the lifetime broadening of all states is 6000 cm^{-1}.
372 This choice satisfactorily reproduced the experimental spectrum of the 2,1,3–benzothiadiazole
373 derivative.[86] Values of the TPA cross-sections are on the order of 10^4 GM. The largest peaks
374 in the TPA spectrum appear in the region 400–470 nm, corresponding to the strongest one–
375 photon absorptions of the [60]fullerene moiety which occur in the region 200–235 nm. From
376 Figs. **??–??** we see that the largest TPA cross section for **3** is almost an order of magnitude
377 greater than that of the other systems. Likewise, the $\mathrm{Re}\overline{\gamma}$ value for **3** (as opposed to $\mathrm{Im}\overline{\gamma}$,
378 which determines TPA) is much larger than the corresponding value for **1** and **2** (see Table
379 6).

380 ## 4.4   Vibrational contributions to electric (hyper)polarizabilities

381 In this section, we present our results for vibrational contributions to the average (hy-
382 per)polarizabilities calculated at the HF/6-31G level of theory for **1**, **2**, **3** and **8** as well as

383 for the chromophores **5**, **6** and **7**. As mentioned previously, the geometries used were opti-
384 mized at the same level of theory, *i.e.* HF/6-31G. Due to computational limitations these
385 calculations were limited to the double harmonic approximation except for **8**. For all the
386 properties considered here except static β the NR treatment is identical to the double har-
387 monic approximation. For the static β a first-order perturbation correction due to electrical
388 and mechanical anharmonicity is included in NR as well. The NR calculations were carried
389 out fully numerically.
390
391 In the case of **8** we focused on the Cartesian x direction to obtain a preliminary assess-
392 ment of the magnitude of the NR contribution. This direction, which is parallel to the N–H
393 bond of the pyrrolidine ring, corresponds to the largest (in magnitude) diagonal component
394 of the purely electronic β at the Hartree–Fock level of theory. It was found that the static
395 $\alpha_{xx}^{nr} = 11.78$ a.u. is much smaller than the electronic counterpart (501.28 a.u.). However,
396 the opposite is true for the static first hyperpolarizability since the electronic β_{xxx}^{e} is -35.8
397 a.u. whereas $\beta_{xxx}^{nr} = $ -608.7 a.u. The contribution of the harmonic term $[\mu\alpha]^{(0,0)}$ is only
398 128.7 a.u. and, thus, it is clear that the first–order anharmonic terms $[\mu^3]^{(0,1)}$ and $[\mu^3]^{(1,0)}$
399 are much more important. Adopting the infinite optical frequency approximation,[59], which
400 is known to be accurate at typical measurement frequencies, $\beta_{xxx}^{nr}(-\omega;\omega,0)_{\omega\to\infty}$ is 1/3 the
401 static double harmonic value or 42.9 a.u. Within the same infinite optical frequency approx-
402 imation $\gamma_{xxxx}^{nr}(-2\omega;\omega,\omega,0)_{\omega\to\infty} = \frac{1}{4}[\mu\beta]^{(0,0)} = $ -40 a.u. In this case the value is quite small
403 compared to the electronic $\gamma_{xxxx}^{e} = 40201$ a.u.
404
405 The vibrational contributions for **1**, **2**, **3**, **5 6**, **7** and **8**, calculated using the double–harmonic
406 oscillator approximation, are presented in Table 7. For β the double harmonic approximation
407 is meaningful as far as the dc–Pockels effect is concerned, but is too crude an approximation
408 to be useful for the static β as we have seen. Thus the quantity $[\mu\alpha]^{(0,0)}$ is listed in the
409 table solely for convenience; it is exacly three times the dc–Pockels β. The nuclear relax-
410 ation contribution to γ for the intensity dependent refractive index process are also given in
411 Table 7 together with the electronic contributions to second hyperpolarizability. The results
412 reported in Table 7 were done seminumerically, *i.e.* second derivatives of the energy (vibra-
413 tional force constant matrix) were obtained by differentiation of analytical first derivatives.
414 Thus, the comparison of these results with those discussed above may be additionally used
415 as a reference to assess the magnitude of the numerical errors. The difference in the x com-
416 ponent of the $[\mu\alpha]^{(0,0)}$ term was found to be 11% and much smaller for $[\mu^2]^{(0,0)}$.
417
418 From Table 7 the average static vibrational polarizability of **1** and **2** are similar in mag-
419 nitude whereas the value for **3** is several times larger. For the latter, the chromophore **7**
420 makes the dominant contribution. In each case, however, the vibrational contribution is
421 small compared to the electronic term. The three molecules **1**, **2**, and **3**) give similar values
422 for the dc–Pockels effect and the overwhelmingly dominant contribution in the case of **1**
423 and **2** arises because of the additional presence of the [60]fullerene moiety. Furthermore, the
424 averaged vibrational term is substantially larger than the corresponding static electronic
425 first hyperpolarizability at the HF/6-31G level. In the case of second hyperpolarizability,
426 however, the electronic contributions seem to be of either similar or larger magnitude than
427 the $\overline{\gamma}^{nr}(-\omega;\omega,-\omega,\omega)_{\omega\to\infty}$ term. Based on the preliminary calculations for molecule **8** the
428 total vibrational contribution may be even much more important as compared to the elec-
429 tronic term. Of course, it should be borne in mind that the effect of electron correlation,
430 which has not been considered in the present study, could significantly reduce the calculated
431 vibrational value.[87,88]

5   Conclusions

In this paper we have performed an extensive analysis of electronic and vibrational contributions to molecular (hyper)polarizabilities for several recently synthesized [60]fullerene derivatives. It has been found that the 60[fullerene] moiety, acting as an electron acceptor in the ground electronic state, significantly enhances the average static (hyper)polarizabilities. Modification of the [60]fullerene–benzothiazole system by adding a triphenylamine moiety (molecule **3**) increases the average static electronic first and second hyperpolarizabilities by roughly a factor of 3 and 2 respectively. The same is true for the major diagonal component except that the factors are even larger. Based on HF/6-31G calculations the vibrational nuclear relaxation contribution to the dc–Pockels β is substantially larger than the static electronic value for all [60]fullerene–chromophore dyads that were studied. At the double harmonic level of approximation the static vibrational β is three times larger and there are indications that anharmonicity contributions may dwarf the double harmonic term. Clearly, the role of anharmonicity in the vibrational NLO properties of organofullerenes deserves further attention.

The especially large second hyperpolarizability of molecule **3** is reflected in its large two–photon absorption in the 400–470 nm region, which corresponds to the strongest one–photon absorption (200–235 nm region) of the [60]fullerene moiety. Large absorption intensities are associated, at least in part, with the fact that the [60]fullerene moiety switches from being an electron acceptor in the ground state to an electron donor in certain excited states.

Due to the size of the molecules studied here the computational methods employed were necessarily restricted. In order to obtain reliable results extensive calibrations were carried out using a hierarchy of methods including HF, MP2 and DFT as well as semiempirical techniques (PM3 and GRINDOL). Linear scaling approaches were also utilized to lower the computational cost. As part of the calibration we found that the effect of electon correlation on β is important. However, DFT calculations using current–DFT, KLI, and a wide variety of conventional functionals all substantially overestimate β. Only the recently developed long–range corrected functionals were successful. Further exploration using several model [60]fullerenes revealed that the large overshoot is connected with the electron–donating capability of the substituent.

6   Acknowledgment

References

[1] (a) Cui, L.; Zhao Y. *Chem. Mater.* **2004**, *16*, 2076. (b) Haider, J. M.; Pikramenou, Z. *Chem. Soc. Rev.* **2005**, *34*, 120. (c) Sun, X.; Liu, Y.; Xu, X.; Yang, C.; Yu, G.; Chen, S.; Zhao, Z.; Qiu, W.; Li, Y.; Zhu, D. *J. Phys. Chem. B* **2005**, *109*, 10786. (d) Rahman, G. M. A.; Guldi, D. M.; Cagnoli, R.; Mucci, A.; Schenetti, L.; Vaccari, L.; Prato, M. *J. Am. Chem. Soc.* **2005**, *127*, 10051. (e) Guo, Z.; Du, F.; Ren, D.; Chen, Y.; Zheng, J.; Liu, Z.; Tian, J. *J. Mater. Chem.* **2006**, *16*, 3021. (f) Jiang, L.; Li, Y. *J. Porphyrins and Phtalocyanines* **2007**, *11*, 299.

[2] Kanis, D.R.; Ratner, M. A.; Marks, T. J. *Chem. Rev.* **1994**, *94*, 195.

[3] Bartkowiak, W. In *Non–Linear Optical Properties of Matter. From Molecules to Condensed Phases*, Papadopoulos, M.; Sadlej, A. J.; Leszczynski, J., Eds.; Springer, 2006.

[4] Morrall, J. P. L.; Humphrey, M. G.; Dalton, G. T.; Cifuentes, M. P.; Samoc, M. In *Non–Linear Optical Properties of Matter. From Molecules to Condensed Phases*, Papadopoulos, M.; Sadlej, A. J.; Leszczynski, J., Eds.; Springer, 2006.

[5] Coe, B. J. In *Non–Linear Optical Properties of Matter. From Molecules to Condensed Phases*, Papadopoulos, M.; Sadlej, A. J.; Leszczynski, J., Eds.; Springer, 2006.

[6] Oudar, J. L.; Chemla, D. S. *J. Chem. Phys.* **1977**, *66*, 2664.

[7] (a) Liddell, P. A.; Kuciauskas, D.; Sumida, J. P.; Nash, B.; Nguyen, D.; Moore, A. L.; Moore, T. A.; Gust, D. *J. Am. Chem. Soc.* **1997**, *119*, 1400. (b) Imahori, H.; Yamada, K.; Hasegawa, M.; Taniguchi, S.; Okada, T.; Sakata, Y. *Angew. Chem., Inter. Ed. Eng.* **1997**, *36*, 2626. (c) Luo, C.; Guldi, D. M.; Imahori, H.; Tamaki, K.; Sakata, Y. *J. Am. Chem. Soc.* **2000**, *122*, 6535. (d) Imahori, H.; Tamaki, K.; Guldi, D. M.; Luo, C.; Fujitsuka, M.; Ito, O.; Sakata, Y.; Fukuzumi, S. *J. Am. Chem. Soc.* **2001**, *123*, 2607. (e) Imahori, H.; Guldi, D. M.; Tamaki, K.; Yoshida, Y.; Luo, C.; Sakata, Y.; Fukuzumi, S. *J. Am. Chem. Soc.* **2001**, *123*, 6617. (f) Imahori, H.; Tamaki, K.; Guldi, D. M.; Luo, C.; Fujitsuka, M.; Ito, O.; Sakata, Y.; Fukuzumi, S. *J. Am. Chem. Soc.* **2001**, *123*, 2607. (g) Imahori, H.i; Tamaki, K.; Araki, Y.; Sekiguchi, Y.; Ito, O.; Sakata, Y.; Fukuzumi, S. *J. Am. Chem. Soc.* **2002**, *124*, 5165. (h) Liddell, P. A.; Kodis, G.; Moore, A. L.; Moore, T. A.; Gust, D. *J. Am. Chem. Soc.* **2002**, *124*, 7668.

[8] (a) Martin, N.; Sánchez, L.; Herranz, M. A. Guldi, D. M. *J. Phys. Chem. A* **2000**, *104*, 4648. (b) Herranz, M. A.; Ollescas, B., Martin, N.; Luo, C.; Guldi, D. M. *J. Org. Chem.* **2000**, *65*, 5728. (c) Martin, N.; Sanchez, L.; Guldi, D. M. *Chem. Commun.* **2000**, 113. (d) Martin, N.; Sanchez, L.; Illescas, B.; Gonzalez, S.; Herranz, M. A.; Guldi, D. M. *Carbon* **2000**, *38*, 1577. (e) Martin, N.; Sanchez, L.; Guldi, D. M. *Chem. Commun.* **2000**, 113. (f) Allard, E.; Cousseau, J.; Oruduna, J.; Garin, J.; Luo; H.; Araki, Y.; Ito, O. *Phys. Chem. Chem. Phys.* **2002**, *4*, 5944. (g) Kreher, D.; Hudhomme, P.; Gorgues, A.; Luo; H.; Araki, Y.; Ito, O. *Phys. Chem. Chem. Phys.* **2003**, *5*, 4583. (h) Sanchez, L.; Perez, I.; Martin, N.; Guldi, D. M. *Chem. Eur. J.* **2003**, *9*, 2457.

[9] (a) Guldi, D. M.; Maggini, M.; Scorrano, G.; Prato, M. *J. Am. Chem. Soc.* **1997**, *119*, 974. (b) D'Souza, F.; Zandler, M. E.; Smith, P. M.; Deviprasad, G. R.; Arkady, K.; Fujitsuka, M.; Ito, O. *J. Phys. Chem. A* **2002**, *106*, 649. (c) Zandler, M. E.; Smith, P. M.; Fujitsuka, M.; Ito, O.; D'Souza, F. *J. Org. Chem.* **2002**, *67*, 9122. (d) Fujitsuka, N.; Tsuboya, R.; Hamasaki, M.; Ito, S.; Onodera, S.; Ito, O.; Yamamoto, Y. *J. Phys. Chem. A* **2003**, *107*, 1452.

[10] Sandanayaka, A. S. D.; Matsukawa, K.; Ishi-I, T.; Mataka, S.; Araki, Y.; Ito, O. *J. Phys. Chem. B* **2004**, *108*, 19995.

[11] Zeng, H. -P.; Wang, T.; Sandanayaka, A. S. D.; Araki, Y.; Ito, O. *J. Phys. Chem. A* **2005**, *109*, 4713.

[12] (a) Hogel, H. *J. Phys. Chem.* **1965**, *69*, 755. (b) Pai, D. M. *J. Chem. Phys.* **1970**, *52*, 2285. (c) Wang, Y. *Nature* **1992**, *356*, 585. (d) Wang, Y.; Suna, A. *J. Phys. Chem. B* **1997**, *101*, 5627.

[13] (a) Raimundo, J.-M.; Blanchard, P.; Brisset, H.; Akoudad, S.; Roncali, J. *Chem. Commun.* **2000**, 939. (b) Akhtaruzzaman, M.; Tomura, M.; Zaman, M. B.; Nishida, J.; Yamashita, Y. *J. Org. Chem.* **2002**, *67*, 7813. (c) Edelmann, M. J.; Raimundo, J.-M.; Utesch, N. F.; Diederich, F.; Boudon, C.; Gisselbrecht, J.-P.; Gross, M. *Helv. Chim. Acta* **2002**, *85*, 2195.

[14] Thomas, K. R. J.; Lin, M. Velusamy, J. T.; Tao, Y.-T.; Chuen, C.-H. *Adv. Funct. Mater.* **2004**, *14*, 83.

[15] (a) Sandanayaka, A. S. D.; Sasabe, S.; Araki, Y.; Furosho, Y.; Ito, O.; Takata, T. *J. Phys. Chem. A*, **2004**, *108*, 5145. (b) Sandanayaka, A. S. D. Taguri, Y.; Araki, Y.; Ishi-I, T.; Mataka, S.; Ito, O. *J. Phys. Chem. B* **2005**, *109*, 22502. (c) Borsenberger, P. M.; Fitzgerald, J. J. *J. Phys. Chem.* **1993**, *97*, 4815. (d) Adachi, Ch.; Nagai, K.; Tamoto, N. *Appl. Phys. Lett.* **1995**, *66*, 2679. (e) Shirota, Y. *J. Mater. Chem.* **2005**, *15*, 75.

[16] Krieg, T.; Petr, A.; Barkleit, G.; Dunsch, L. *Appl. Phys. Lett.* **1999**, *74*, 3639 and references therein.

[17] (a) Tagmatarchis, N.; Prato, M. *Synlett.* **2003**, 768. (b) Tagmatarchis, N.; Prato, M. *Struct. Bonding* **2004**, *109*, 1.

[18] Göppert-Mayer, M. *Ann. Phys.* **1931**, *9*, 273.

[19] Albota M.; Beljonne D.; Brédas J. -L.; Ehrlich J. E.; Fu, J. -Y.; Heikal, A. A.; Hess, S. E.; Kogej, T.; Levin, M. D.; Marder, S. R.; McCord–Maughon, D.; Perry, J. W.; Röckel, H.; Rumi, M. *Science* **1998**, *281*, 1653.

[20] Kogej, T.; Beljonne, D.; Meyers, F.; Perry, J. W.; Marder, S. R.; Brédas, J. L. *Chem. Phys. Lett.* **1998**, *298*, 1.

[21] Norman, P.; Luo, Y.; Ågren, H. *J. Chem. Phys.* **1999**, *111*, 7758.

[22] Macak, P.; Luo, Y.; Norman, P.; Ågren, H. *J. Chem. Phys.* **2000**, *113*, 7055.

[23] Lee, W. -H.; Lee, H.; Kim, J. -A.; Choi, J. -H.; Cho, M.; Jeon, S. -J.; Cho, B. R. *J. Am. Chem. Soc.* **2001**, *123*, 10658.

[24] Zhou, X.; Ren, A. -M.; Feng, J. -K.; Liu, X. -J.; Zhang, J.; Liu, J. *Phys. Chem. Chem. Phys.* **2002**, *4*, 4346.

[25] Liu, X. -J.; Feng, J. -K.; Ren A. -M.; Zhou, X. *Chem. Phys. Lett.* **2003**, *373*, 197.

[26] Bartkowiak, W.; Zaleśny, R.; Leszczynski, J. *Chem. Phys.* **2003**, *287*, 103.

[27] Masunov, A.; Tretiak, S. *J. Phys. Chem. B* **2004**, *108*, 899.

[28] Ehrlich, J. E.; Wu, X. L.; Lee, I. Y. S.; Hu, Z. Y.; Röckel, H.; Marder, S. R.; Perry, J. W. *Opt. Lett.* **1997**, *22*, 1843.

[29] Parthenopoulos, D. M.; Rentzepis, P. M. *Science* **1989**, *245*, 843.

[30] Li, X. -D.; Cheng, W. -D.; Wu, D. -S.; Lan, Y. -Z.; Zhang, H.; Gong, Y. -J.; Li, F. -F.; Shen, J. *J. Phys. Chem. B* **2005**, *109*, 5574.

[31] Padmawar, P. A.; Rogers, J. E.; He, G. S.; Chiang, L. Y.; Tan, L. -S.; Canteenwala, T.; Zheng, Q.; Slagle, J. E.; McLean, D. G.; Fleitz, P. A.; Prasad, P. N. *Chem. Mater.* **2006**, *18*, 4065.

[32] Bishop, D. M.; Norman, P. In *Handbook of Advanced Electronic and Photonic Materials and Devices*, Nalwa, H. S., Ed.; Academic Press: San Diego, 2001 and references therein.

[33] Christiansen, O.; Coriani, S.; Gauss, J.; Hättig, C.; Jørgensen, P.; Pawłowski, F.; Rizzo, A. In *Non–Linear Optical Properties of Matter. From Molecules to Condensed Phases*, Papadopoulos, M.; Sadlej, A. J.; Leszczynski, J., Eds.; Springer, 2006.

[34] Champagne, B.; Perpète, E. A.; van Gisbergen, S. J. A.; Baerends, E. -J.; Snijders, J. G.; Soubra–Ghaoui, C.; Robins, K. A.; Kirtman, B. *J. Chem. Phys.* 1998, *109*, 10489.

[35] Champagne, B.; Perpète, E. A.; Jacquemin, D.; van Gisbergen, S. J. A.; Baerends, E. -J.; Soubra–Ghaoui, C.; Robins, K. A.; Kirtman, B. *J. Phys. Chem. A* **2000**, *104*, 4755.

[36] Iikura, H.; Tsuneda, T.; Yanai, T.; Hirao, K. *J. Chem. Phys.* **2001**, *115*, 3540.

[37] Kamiya, M.; Sekino, H.; Tsuneda, T.; Hirao, K. *J. Chem. Phys.* **2005**, *122*, 234111.

[38] Sekino, H.; Maeda, Y.; Kamiya, M.; Hirao, K. *J. Chem. Phys.* **2007**, *126*, 014107.

[39] Yanai, T.; Tew, D. P.; Handy, N. C. *Chem. Phys. Lett.* **2004**, *393*, 51.

[40] Rudberg, E.; Sałek, P.; Helgaker, T.; Ågren, H. *J. Chem. Phys.* **2005**, **123**, 184108.

[41] Dałek, P.; Ågren, H.; Baev, A.; Prasad, P. N. *J. Phys. Chem. A* **2005**, *109*, 11037.

[42] Jacquemin, D.; Perpète, E. A.; Medved', M.; Scalmani, G.; Frisch, M. J.; Kobayashi, R.; Adamo, C. *J. Chem. Phys.* **2007**, *126*, 191108.

[43] Stewart, J. J. P *J. Comp. Chem.* **1989**, *10*, 209.

[44] Stewart, J. J. P *J. Comp. Chem.* **1989**, *10*, 221.

[45] Greengard L.; Rokhlin, V. *J. Comput. Phys.* **1987**, *73*, 325.

[46] Schmidt K. E.; Lee, M. A. *J. Stat. Phys.* **1991**, *63*, 1223.

[47] Millam J. M.; Scuseria, G. E.; *J. Chem. Phys.* **1997**, *106*, 5569.

[48] Frisch, M. J.; Trucks, G. W.; Schlegel, H. B.; Scuseria, G. E.; Robb, M. A.; Cheeseman; J. R.; Montgomery, Jr., J. A.; Vreven, T.; Kudin, K. N.; Burant, J. C.; Millam, J. M.; Iyengar, S. S.; Tomasi, J.; Barone, V.; Mennucci, B.; Cossi, M.; Scalmani, G.; Rega, N.; Petersson, G. A.; Nakatsuji, H.; Hada, M.; Ehara, M.; Toyota, K.; Fukuda, R.; Hasegawa, J.; Ishida, M.; Nakajima, T.; Honda, Y.; Kitao, O.; Nakai, H.; Klene, M.; Li, X.; Knox, J. E.; Hratchian, H. P.; Cross, J. B.; Bakken, V.; Adamo, C.; Jaramillo, J.; Gomperts, R.; Stratmann, R. E.; Yazyev, O.; Austin, A. J.; Cammi, R.; Pomelli, C.; Ochterski, J. W.; Ayala, P. Y.; Morokuma, K.; Voth, G. A.; Salvador, P.; Dannenberg, J. J.; Zakrzewski, V. G.; Dapprich, S.; Daniels, A. D.; Strain, M. C.; Farkas, O.; Malick, D. K.; Rabuck, A. D.; Raghavachari, K.; Foresman, J. B.; Ortiz, J. V.; Cui, Q.; Baboul, A. G.; Clifford, S.; Cioslowski, J.; Stefanov, B. B.; Liu, G.; Liashenko, A.; Piskorz, P.; Komaromi, I.; Martin, R. L.; Fox, D. J.; Keith, T.; Al-Laham, M. A.; Peng, C. Y.; Nanayakkara, A.; Challacombe, M.; Gill, P. M. W.; Johnson, B.; Chen, W.; Wong, M. W.; Gonzalez, C.; Pople, J. A. *Gaussian 03*, Rev. D02, Gaussian, Inc., Wallingford, CT, 2004.

[49] Willets, A.; Rice, J. E.; Burland, D. M.; Shelton, D. P. *J. Chem. Phys.* **1992**, *97*, 7590.

[50] Bishop, D. M.; Kirtman, B.; Champagne, B. *J. Chem. Phys.* **1997**, *107*, 5780.

[51] Luis, J. M.; Marti, J.; Duran, M.; Andres, J. L.; Kirtman, B. *J. Chem. Phys.* **1998**, *108*, 4123.

[52] Kurtz, H. A.; Stewart, J. J. P.; Dieter, K. M. *J. Comp. Chem.* **1990**, *11*, 82.

[53] Quarteroni, A.; Sacco, R.; Saleri, F. *Méthodes Numériques*; Springer–Verlag Italia, Milano, 2007.

[54] MOPAC2007, J. J. P. Stewart Computational Chemistry, Version 7.221L web: HTTP://OpenMOPAC.net

[55] (a) te Velde, G.; Bickelhaupt, F. M.; van Gisbergen, S. J. A.; Fonseca Guerra, C.; Baerends, E. J.; Snijders, J. G.; Ziegler, T. *J. Comput. Chem.* **2001**, *22*, 931. (b) Fonseca Guerra, C.; Snijders, J. G.; te Velde, G.; Baerends, E. J. *Theor. Chem. Acc.* **1998**, *99*, 391. (c) ADF2007.01, SCM, Theoretical Chemistry, Vrije Universiteit, Amsterdam, The Netherlands, http://www.scm.com

[56] DALTON, a molecular electronic structure program, Release 2.0 (2005), see http://www.kjemi.uio.no/software/dalton/dalton.html

[57] Schmidt, M. W.; Baldridge, K. K.; Boatz, J. A.; Elbert, S. T.; Gordon, M. S.; Jensen, J. H.; Koseki, S.; Matsunaga, N.; Nguyen, K. A.; Su, S.; Windus, T. L.; Dupuis, M.; Montgomery, J. A. *J. Comput. Chem.* **1993**, *14*, 1347.

[58] Luis, J. M.,; Duran, M.; Champagne, B.; Kirtman, B. *J. Chem. Phys.* **2000**, *113*, 5203.

[59] Kirtman, B.; Champagne, B.; Luis, J. M. *J. Comp. Chem.* **2000**, *21*, 1572.

[60] Bishop, D. M. *Adv. Chem. Phys.* **1998**, *104*, 1.

[61] Kirtman, B.; Luis, J. M. *J. Phys. Chem. A* **2008**, *128*, 114101.

[62] Champagne, B.; Kirtman, B. In *Handbook of Advanced Electronic and Photonic Materials and Devices*, Nalwa, H. S., Ed.; Academic Press: San Diego, 2001 and references therein.

[63] Monson, P. R.; McClain, W. M. *J. Chem. Phys.* **1970**, *53*, 29.

[64] Bartkowiak, W.; Lipiński, J. *J. Phys. Chem. A* **1998**, *102*, 5236.

[65] Lipiński, J.; Bartkowiak, W. *Chem. Phys.* **1999**, *245*, 263.

[66] Bishop, D. M.; Luis, J. M.; Kirtman, B. *J. Chem. Phys.* **2002**, *116*, 9729.

[67] Hedberg, K.; Hedberg, L.; Bethune, D.; Brown, C.; Johnson, R.; de Vries, M. *Science* **1991**, *254*, 410.

[68] Loboda, O.; Jensen, V. R.; Borve, K. J. *Fullerenes, Nanotubes and Carbon Nanostructures* **2006**, *14*, 365.

[69] J. B. Foresman; Æ. Frisch *Exploring Chemistry with Electronic Structure Methods*, Second Edition; Gaussian, Inc., Pittsburgh, PA.

[70] van Gisbergen, S. J. A.; Schipper, P. R. T.; Gritsenko, O. V.; Baerends, E. J.; Snijders, J. G.; Champagne, B.; Kirtman, B. *Phys. Rev. Lett.* **1999**, *83*, 694.

[71] Champagne, B.; Perpete, E. A. *Int. J. Quant. Chem.* **1999**, *75*, 441.

[72] van Faassen, M.; de Boeij, P. L.; van Leeuwen, R.; Berger, J. A.; Snijders, J. G. *Phys. Rev. Lett.* **2002**, *88*, 186401.

[73] Krieger, J. B.; Li, Y.; Iafrate, G. J. *Phys. Rev. A* **1992**, *45*, 101.

[74] Vignale, G.; Kohn, W. *Phys. Rev. Letters* **1996**, *77*, 2037.

[75] Kirtman, B.; Bonness, S.; Ramirez-Solis, A.; Champagne, B.; Matsumoto, H.; Sekino, H. *J. Chem. Phys.* **2008**, *128*, 114108.

[76] Kümmel, S.; Kronik, L.; Perdew, J. P. *Phys. Rev. Lett.* **2004**, *93*, 213002.

[77] B. Champagne, Bulat, F. A.; Yang, W.; Bonness, S.; Kirtman, B. *J. Chem. Phys.* **2006**, *125*, 194114.

[78] Bulat, F. A.; Toro-Labbé, A.; Champagne, B.; Kirtman, B.; Yang, W. *J. Chem. Phys.* **2005**, *123*, 014319.

[79] Lipiński, J. *Int. J. Quant. Chem.* **1988**, *34*, 423.

[80] Lipiński, J.; Bartkowiak, W. *J. Phys. Chem. A* **1997**, *101*, 2159.

[81] Maggini, M.; Scorrano, G. *J. Am. Chem. Soc.* **1993**, *115*, 9798.

[82] Dirk, C .W.; Cheng, L. -T.; Kuzyk, M. G. *Int. J. Quant. Chem.* **1992**, *43*, 27.

[83] Cronstrand P.; Luo Y.; Ågren, H. *Chem. Phys. Lett.* **2002**, *352*, 262.

[84] Zaleśny, R.; Bartkowiak, W.; Styrcz, S.; Leszczynski J. *J. Phys. Chem. A* **2002**, *106*, 4032.

[85] Hamasaki, R.; Ito, M.; Lamrani, M.; Mitsuishi, M.; Miyashita, T.; Yamamoto, Y. *J. Mater. Chem.* **2003**, *13*, 21.

[86] Kato, S. -I.; Matsumoto, T.; Ishi-i, T.; Thiemann, T.; Shigeiwa, M.; Gorohmaru, H.; Maeda, S.; Yamashita, Y.; Mataka, S. *Chem. Commun.* **2004**, 2342.

[87] Torrent–Sucarrat, M.; Solà, M.; Duran, M.; Luis, J. M.; Kirtman, B. *J. Chem. Phys.* **2003**, *118*, 711.

[88] Zaleśny, R.; Bartkowiak, W.; Toman, P.; Leszczynski, J. *Chem. Phys.* **2007**, *337*, 77.
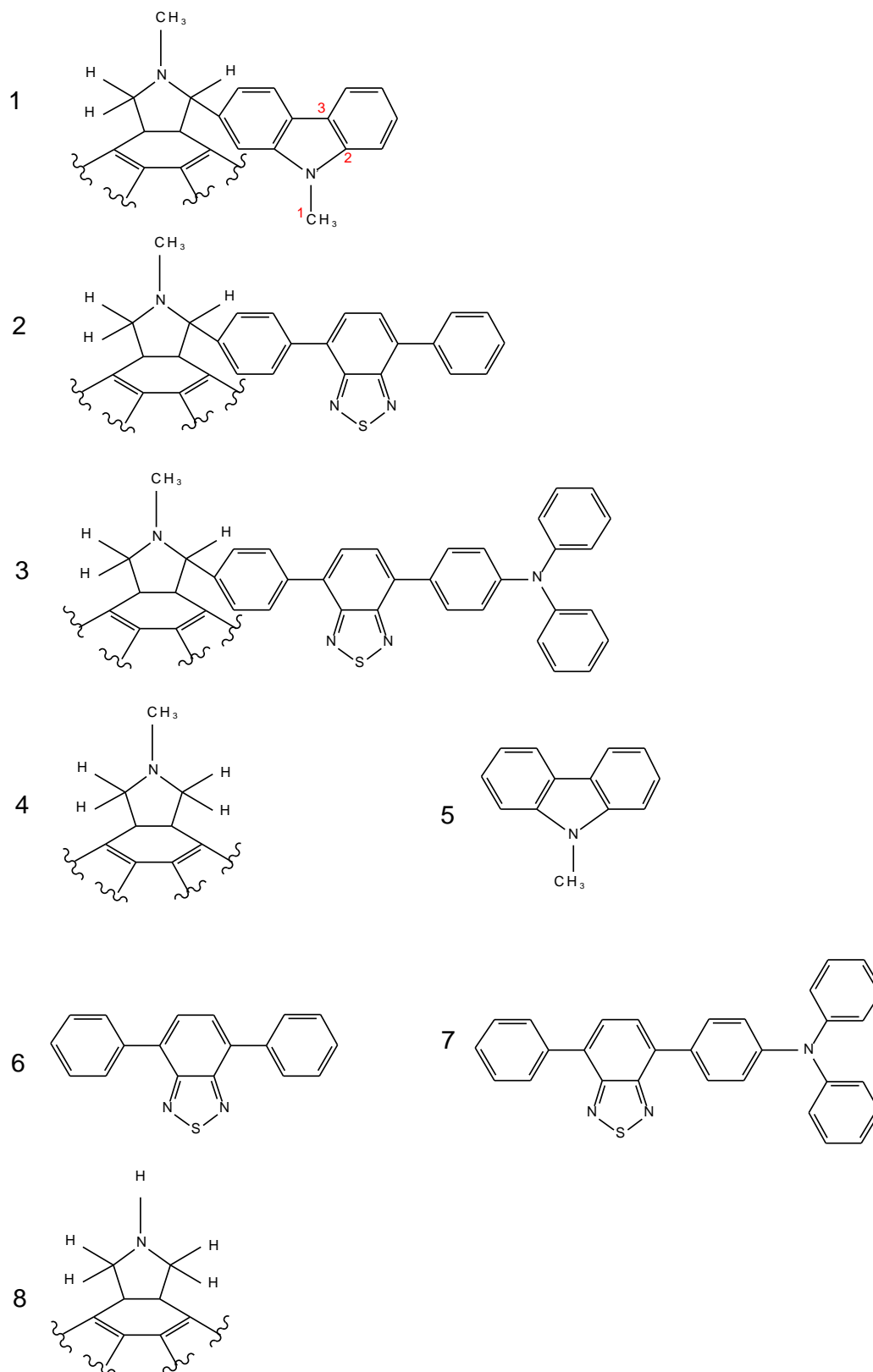
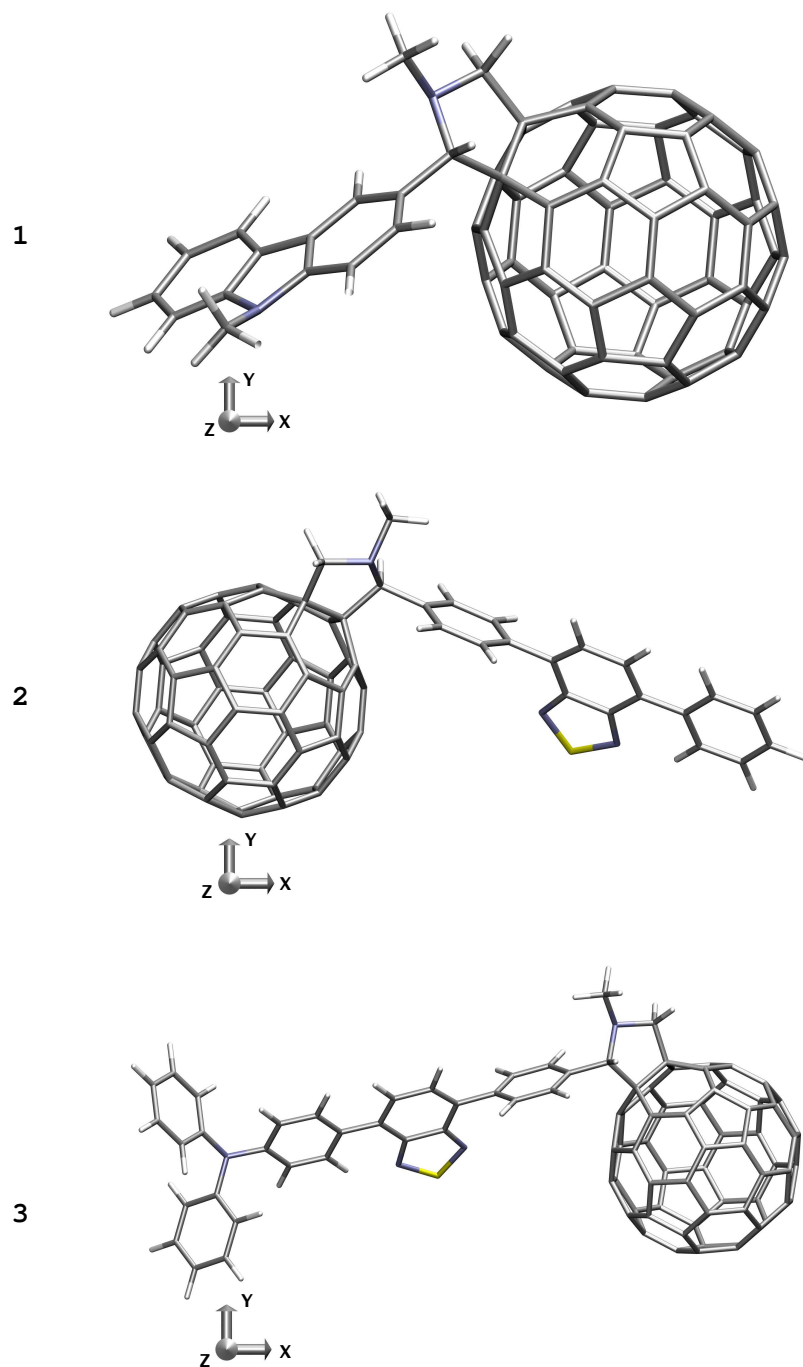Figure 1: Schematic representation of investigated molecules

Figure 2: Structure of investigated [60]fullerene derivatives. Shown is the orientation of cartesian directions used in property calculations.
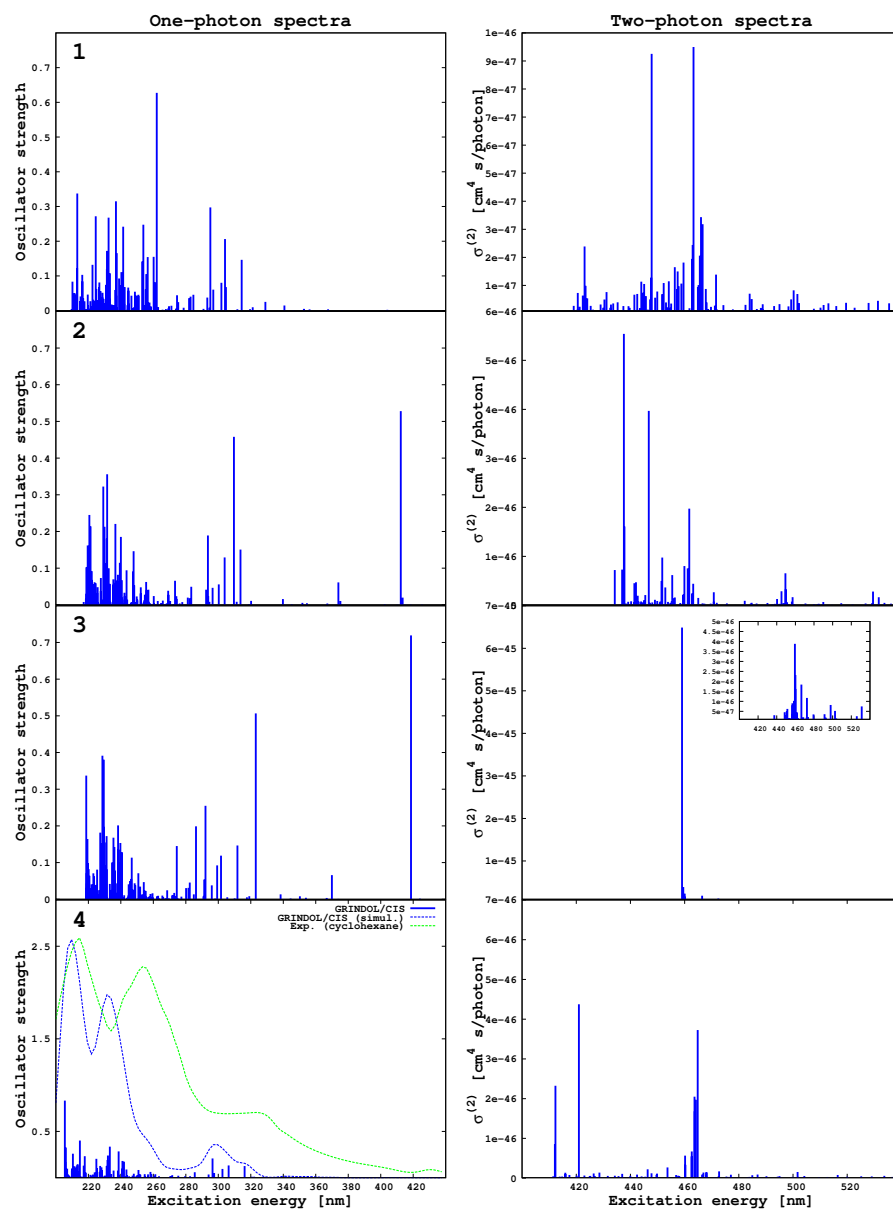
Figure 3: One– and two–photon excitation spectra for molecules **1–4**. The inset figure presents the TPA spectrum at reduced scale so that the weaker transitions can be seen.
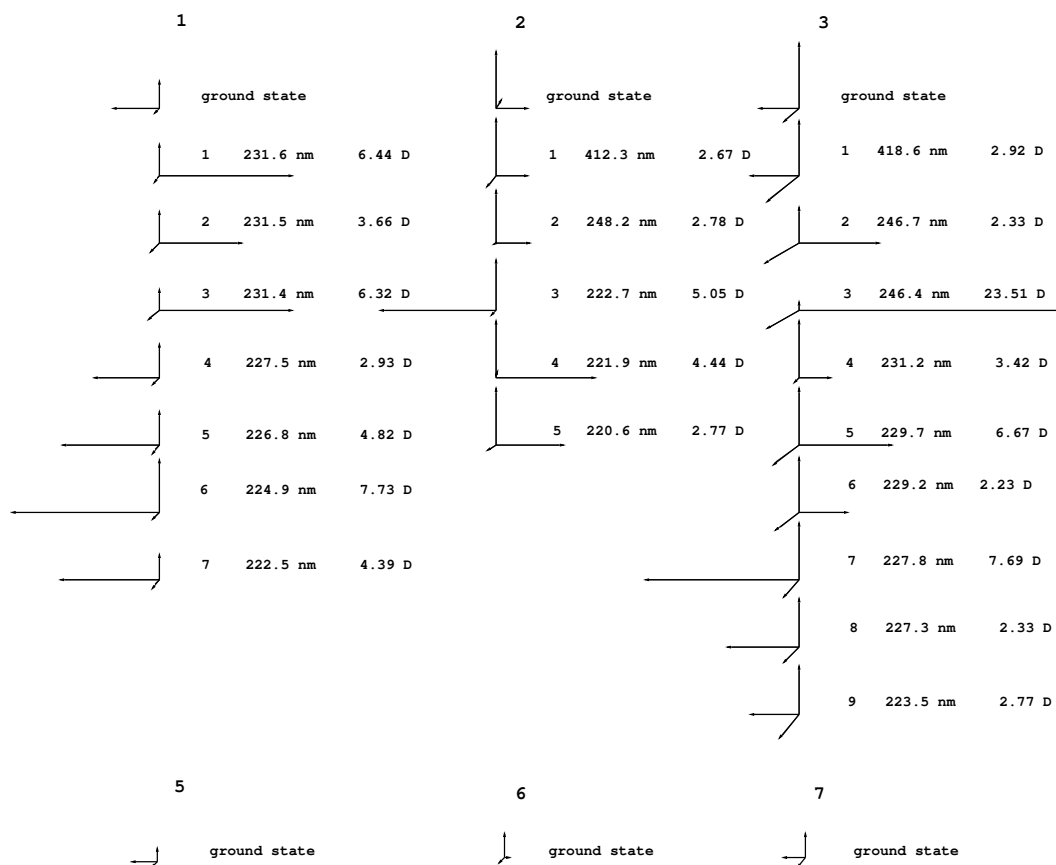
Figure 4: Schematic representation of dipole moment components in the ground and selected excited states (see text for explanation) for **1**, **2** and **3**, respectively. Ground state dipole moment components for **5**, **6** and **7** are presented as well. The components refers to the orientation of molecules presented in Fig. 2. Shown also are the excitation energies and the magnitude of the difference in dipole moment between the given excited state and the ground state.

Table 1: Geometrical parameters of **1** calculated using the PM3 method and at the B3LYP/6-31G(d) level of theory. N' refers to the nitrogen atom located in carbazole moiety. All other parameters refer to the pyrrolidine ring. Distances are given in Å and angles in degrees.

Method	C–C (6–6)	C–CH$_2$	C–CHR	N–CH$_2$	N–CHR	N–CH$_3$	N'–CH$_3$	∠CH$_2$NCH$_3$	∠CN'CH$_3$	∠C1N'C2C3
PM3	1.584	1.537	1.556	1.486	1.500	1.474	1.466	113.8	121.0	149.4
B3LYP	1.611	1.556	1.558	1.452	1.463	1.457	1.447	112.7	125.6	177.8

Table 2: Dipole moment μ and average polarizability $\overline{\alpha}$, first hyperpolarizability $\overline{\beta}$, and second hyperpolarizability $\overline{\gamma}$ of **1** calculated at the HF/6-31G(d) level of theory for the structures optimized using PM3 and B3LYP/6-31G(d). All values are given in atomic units

	PM3 geometry	B3LYP/6-31G(d) geometry
μ	1.72	1.92
$\overline{\alpha}$	634.09	640.33
$\overline{\beta}$	403.33	470.14
$\overline{\gamma}$	71279	70414

Table 3: Calculated diagonal x-component for electronic dipole moment μ_x, linear polarizability (α_{xx}) and first hyperpolarizability (β_{xxx}) of **1**. All values are given in atomic units

Method	μ_x	α_{xx}	β_{xxx}
HF/3-21G	−1.79	681.87	−661.1
HF/6-31G(d)	−1.47	735.27	−558.1
MP2/6-31G(d)	−1.67	782.99	−1301.2
MP2/3-21G	−1.88	719.14	−1525.6
CAM-B3LYP/3-21G	−1.82	719.27	−1671.9
LC-BLYP/3-21G	−1.77	702.79	−1193.4
B3LYP/3-21G	−1.91	758.63	−4484.7
CurDFT/DZP	−2.09	672.05	−5378.5
LB94/DZP	−2.09	901.25	−10291.0
RevPBEx/DZP	−2.42	900.59	−15196.0
GRAC/DZP	−2.64	926.19	−19816.0
PW91/3-21G	−2.19	819.73	−20125.6
KT2/DZP	−2.79	939.00	−22050.0
LDA/3-21G	−2.32	830.09	−22487.0
KT1/DZP	−2.81	948.14	−22541.0
KLI/DZP	−3.65	975.11	−83807.0

Table 4: Values of the dipole moment (μ), average linear polarizability, ($\overline{\alpha}$), and average first hyperpolarizability ($\overline{\beta}$) for several model systems. All values are given in atomic units.
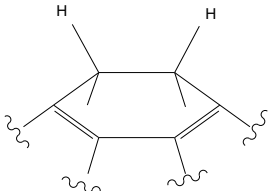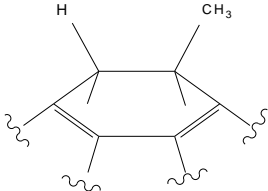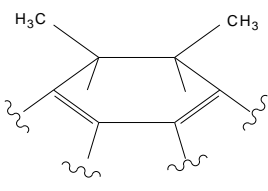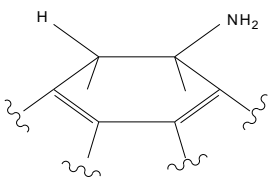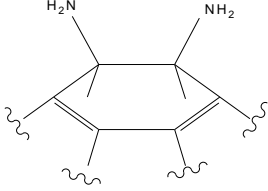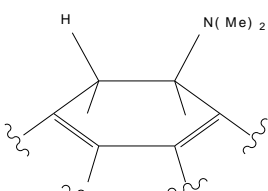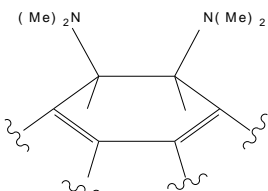
Label	Molecule	μ	$\overline{\alpha}$	$\overline{\beta}$	Method
9		1.00	449.23	-29.0	HF/6-31G(d)
		0.92	479.65	-58.2	BLYP/6-31G(d)
10		1.07	461.00	-18.6	HF/6-31G(d)
		0.98	493.24	-36.0	BLYP/6-31G(d)
11		1.18	472.26	-3.4	HF/6-31G(d)
		1.10	506.32	12.45	BLYP/6-31G(d)
12		1.09	457.12	-29.3	HF/6-31G(d)
		1.01	490.18	81.9	BLYP/6-31G(d)
13		1.21	465.04	-7.5	HF/6-31G(d)
		1.19	501.79	277.2	BLYP/6-31G(d)
14		1.11	481.76	-64.3	HF/6-31G(d)
		1.00	520.46	1019.1	BLYP/6-31G(d)
15		1.33	512.28	-74.8	HF/6-31G(d)
		1.28	562.06	3046.5	BLYP/6-31G(d)

Table 5: The values of dipole moment (μ), first– (α), second– (β) and third–order polarizability (γ) for **1**, **2** and **3**. All values are given in atomic units.

Property	Method	1	2	3
μ_x	HF/3-21G	-1.79	1.09	-1.29
	MP2/3-21G	-1.88	1.00	-1.25
	LC-BLYP/3-21G	-1.77	0.94	-1.22
	PM3	-1.30	0.86	-1.02
α_{xx}	HF/3-21G	681.87	859.68	1051.74
	MP2/3-21G	719.14	867.34	1079.56
	LC-BLYP/3-21G	702.79	874.92	1091.88
	PM3	671.91	858.72	1061.88
β_{xxx}	HF/3-21G	-674.0	664.1	-4552.2
	MP2/3-21G	-1525.6	985.4	-8267.3
	LC-BLYP/3-21G	-1193.3	874.9	-7457.4
	PM3	-1028.2	1373.7	-7400.9
γ_{xxxx}	HF/3-21G	171729	596479	1542361
	MP2/3-21G	384606	988307	3103560
	LC–BLYP/3-21G	291518	826348	2655793
	PM3	261749	1073875	3051099

Table 6: Comparison of average static linear and nonlinear optical properties of **1**, **2**, **3** with the isolated chromophores **5**, **6** and **7**. All values are given in atomic units.

	Method	**1**	**5**	**2**	**6**	**3**	**7**
$\overline{\alpha}$	PM3	591.89	120.75	679.70	202.92	817.79	336.95
$\overline{\beta}$	PM3	546.6	156.8	521.5	84.9	1746.2	794.4
$\overline{\gamma}$	PM3	135377	26794	307890	138123	730346	454142

Table 7: Electronic and vibrational contributions to molecular (hyper)polarizabilities calculated at the HF/6-31G level of theory for **1**, **2**, **3**, **5**, **6**, **7** and **8**. All values are given in atomic units.

	1	**5**	**2**	**6**	**3**	**7**	**8**
$\overline{\alpha}^{nr}$	29.2	4.0	42.2	4.3	119.0	86.6	11.8
$\overline{\alpha}^{e}$	609.6	127.0	695.2	205.7	836.3	339.5	458.6
$\overline{[\mu\alpha]}^{(0,0)}$	3037.0	50.1	5660.1	74.9	4590.4	7329.1	160.8
$\overline{\beta}^{nr}(-\omega;\omega,0)_{\omega\to\infty}$	1012.0	16.7	1886.7	25.0	1530.1	2443.0	53.6
$\overline{\beta}^{e}$	288.2	89.9	-51.8	-25.5	835.8	268.0	-4.0
$\overline{\gamma}^{nr}(-\omega;\omega,-\omega,\omega)_{\omega\to\infty}$	48637	5702	155719	25818	293915	133909	19437
$\overline{\gamma}^{e}$	67158	12189	151985	56683	361605	175522	26880